Title

# Theoretical Analysis Of A Novel Integrated Energy System Formed By A Microturbine And A Exhaust Fired Single-Double Effect Absorption Chiller



Journal
International Journal of Thermodynamics, 9(1)

ISSN
1301-9724

Authors
Samuelsen, GS
Medrano, M
Mauzey, JL
et al.

Publication Date
2006-09-10

Int. J. of Thermodynamics
Vol. 9 (No. 1), pp. 29-36, March 2006

ISSN 1301-9724

# Theoretical Analysis of a Novel Integrated Energy System Formed by a Microturbine and an Exhaust Fired Single-Double Effect Absorption Chiller

Marc Medrano*
Department of Industrial Engineering and Computer Sciences;
University of Lleida; Lleida Spain
E-mail: mmedrano@diei.udl.es, phone: (+34) 973702744

Josh Mauzey, Vince McDonell, Scott Samuelsen
Advanced Power and Energy Program, University of California, Irvine

Dieter Boer
Department of Mechanical Engineering; ETSEQ
University of Rovira i Virgili, Tarragona Spain

**Abstract**

Integrated Energy Systems (IES) combine a distributed power generation system (DG) such as a microturbine generator (MTG) or a fuel cell with thermally activated technologies (TAT) such as absorption cooling. This integration maximizes the efficiency of energy use by utilizing on-site most of the waste heat generated by DG, and reduces harmful emissions to the environment. This study investigates the energy and exergy performance of an IES. This system is comprised of an MTG with internal recuperator and a novel absorption cooling cycle. The absorption cycle is a single-double effect exhaust fired cycle, which recuperates the heat exchanged from the MTG exhaust gases using two generators at two different levels of temperature. The selection of the DG element, the TAT element and their internal configurations is based upon a real IES commercial unit that has been tested in the APEP-UCI DG testing facilities in Irvine, California. This unit has an electrical power capacity of 28 kW and a cooling capacity of 14 refrigeration tons (49.2 kW). Inputs for the thermodynamic models developed for the MTG and for the absorption cycle are derived from experimental variables that will be controlled in the testing phase. The MTG model is using empirical correlations for key model parameters (pressure ratio, turbine inlet temperature, etc.) from previous studies in order to predict the observed change in performance with part load operation. The calculated mass flow rate and temperature of the exhaust gases are inputs for the absorption cycle model, together with cooling and chilled water inlet temperatures and flow rates. Heat and mass transfer efficiencies along with heat transfer coefficients for the suite of heat exchangers comprising the single-double effect absorption cycle are determined from proprietary testing data provided by the manufacturers.

*Keywords: Integrated energy systems, distributed generation, thermally activated technologies, microturbine, absorption chiller, exhaust fired chiller, single-double effect absorption cycle*

## 1. Introduction

Integrated Energy Systems (IES) combine a distributed power generation system (DG) such as a microturbine generator (MTG) or a fuel cell with thermally activated technologies (TAT) such as absorption cooling, water heating or desiccant dehumidification. Other acronyms often used in the literature to refer to the same IES concept are CHPB (cooling, heating and power for buildings), BCHP (building cooling, heating and power) and CCHP (combined cooling, heating and power). This integration maximizes the efficiency of

*Author to whom correspondence should be addressed

energy use by utilizing on-site most of the waste heat generated by DG, and subsequently reduces harmful emissions to the environment.

In the past decades the implementation of an IES in a particular facility involved the selection and purchase of the disparate components of an IES (i.e.: the prime mover, the heat exchanger, the chiller), followed by a customized, rather costly installation on-site. However, the current trend of Japanese and US DG manufacturers is to develop pre-engineered packaged units that will significantly reduce costs, boost system efficiency, and simplify the installation process to the point of a plug-and-play process. This integration will likely encourage many building and industry owners to adopt IES rapidly (Engle, 2004). Some integrated products are in the development phase, and a few are already commercial.

The Advanced Power and Energy Program (APEP) at the University of California, Irvine (UCI) has developed a test rig facility in order to test and evaluate the operational and emissions performance of both DG power-only and IES units. After several years of experience with power-only and combined heat and power (CHP) tests of MTGs from several manufacturers (McDonell et al. 2003), the first tests with a CCHP commercial unit were accomplished in 2005 (Nogués et al., 2006). This IES unit is manufactured by Takuma Company, Ltd. for the Japanese market and consists of a 28 kW MTG with recuperator and a novel single-double effect exhaust fired absorption chiller with a cooling capacity of 14 refrigeration tons (49.2 kW) and a nominal coefficient of performance (COP) of 1.

As a first step prior to the test phase, thermodynamic models for the MTG and the chiller integrating characteristics of the commercial unit were developed. The purpose of this paper is to present these models and to investigate the energy and exergy performance of the integrated energy system at different operating conditions.

## 2. Description of the Integrated Energy System to be Tested

The IES commercial unit to be tested consists of an MTG element, a Takuma TCP30 model, and an exhaust fired absorption chiller/heater element, a Takuma EGT-15 model.

The first element is a 30 kW capacity single-shaft turbine with recuperator manufactured by Capstone Turbine Corporation. This assembly uses air bearings, has a rotating speed of 96000 revolutions per min, and has a permanent magnet type high-speed generator (Gillette, 2004).

The absorption chiller/heater is a single-double effect exhaust fired unit with 49.8 kW of heating capacity and 49.2 kW (14 refrigeration tons) of cooling capacity and uses the system water-LiBr as a working fluid mixture. The single-double effect cycle used in this chiller increases the heat exchanged from the MTG exhaust gases using two generators at two different temperature levels. The exhaust gases leaving the high temperature generator of the double effect cycle can then be further utilized to drive the single effect cycle and produce an extra cooling effect.

The exhaust gases from the MTG are directed to the absorption chiller through insulated ducting to minimize losses. *Figure 1* shows a picture of the Takuma IES unit already located in APEP's test facilities. *Figure 2* presents a schematic flowchart with energy fluxes of the MTG and the absorption chiller integrating the unit.

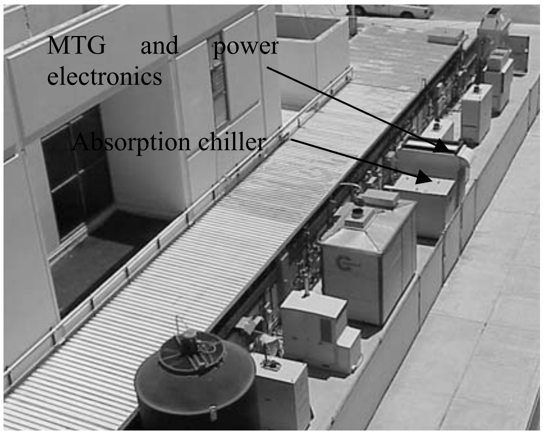


*Figure 1. IES unit installed in APEP's test facilities (4th and 5th units starting from bottom to top of picture).*

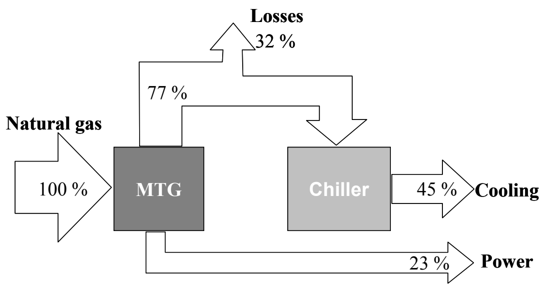


*Figure 2. Sankey diagram of the MTG and the absorption chiller cycle integrating the IES unit working in cooling mode.*

## 3. Microturbine

### 3.1 Thermodynamic cycle

*Figure 3* shows the components of the microturbine generator that are included in the thermodynamic model. The air entering the MTG (state point 1) is compressed in the air compressor to state point 2. Then, air goes to the recuperator, where it is heated by the rejected exhaust gases (state point 3). Air enters with compressed natural gas into the adiabatic combustion chamber. The resulting high temperature combustion gases (state point 4) are then fed to the gas turbine, where they are expanded from state point 4 to state point 5. After the turbine, the rejected gases flow through the recuperator where heat is transferred to incoming air. The temperature of the exhaust gas downstream of the recuperator is still high enough to drive an absorption cycle, as explained in next section.

### 3.2 MTG simulation methodology

A thermodynamic model was developed for the MTG using the program Engineering Equation Solver (EES). Most of the mathematical equations used to describe the cycle can be found elsewhere (Labinov et al., 2002). The combustion process is not treated as a black box, however. The chemical reaction between the fuel and the air in the chamber is modeled and excess air and exhaust gases compositions are obtained. Some input parameters of the cycle (air compressor and turbine isentropic efficiencies, recuperator efficiency, combustor efficiency, and fuel compressor isentropic efficiency) were determined on the basis of manufacturers' data at full load conditions, and were assumed constant for the operating range studied. To account for changes in performance of the MTG unit with part-load operation, some other parameters (i.e. turbine inlet temperature, pressure ratio, recuperator heat loss coefficient, generator heat losses, and controller heat losses) were correlated to net power output using literature experimental data for the same MTG unit (Labinov et al., 2002).

Input data are presented below. The first three parameters will vary during the future experimental testing process and their effect on the performance parameters will be analyzed. The rest are assumed constant for the range of operating conditions investigated:

- Net power output
- Air inlet temperature
- Fuel inlet temperature
- Air compressor isentropic efficiency
- Turbine isentropic efficiency
- Recuperator efficiency
- Combustor efficiency
- Fuel compressor isentropic efficiency
- Inlet compressor pressure

Output data are:

- Pressures, temperatures, gas compositions, mass flows, enthalpies, entropies, exergies of the flows
- Mechanical or thermal power and irreversibility rate of the main components
- Thermal efficiency of MTG based on natural gas higher heating value (HHV)

The principal assumptions of the MTG model are:

- No pressure losses
- No heat losses in turbine, compressors and combustion chamber
- Natural gas is treated as pure methane
- Air, methane and combustion gases are treated as ideal gases

## 4. Absorption Chiller

### 4.1 Thermodynamic cycle

The novel configuration of the single-double effect absorption cycle shown in *Figure 4* combines a series flow double effect cycle with a single effect cycle. Detailed description of the separated cycles can be found elsewhere (Herold et al., 1996).

Both cycles share common components, namely the absorber, the evaporator and the condenser. The single-double effect cycle is comprised of 9 main components. The names of each of the components, the cycle they belong to, and the abbreviations used in *Figure 4* are shown in TABLE I.

The following heat transfers take place with external fluids. Heat is supplied at high temperature (270-280°C) in generator G1 from the exhaust gases exiting the MTG. After G1, the relatively lower temperature gases (160-170°C) supply extra heat in generator G2, which drives the single effect cycle and provides extra cooling (*Figure 5*).

This novel cycle arrangement enables a better utilization of the MTG exhaust gases exergy. Heat is dissipated in absorber A and condenser C to cooling water in a series flow arrangement of cooling water. Chilled water is produced in the evaporator E.

Internal heat is transferred from condensing refrigerant vapor to the absorbent solution in the condenser-generator assembly CG. In the CG, part of the refrigerant is evaporated from the incoming solution on the cold side (state 7 in *Figure 4*). On the hot side superheated refrigerant vapor is condensed (state 18). Between hot and cold solution streams heat is recovered in the solution heat exchangers HPHX1, HPHX2 and LPHX. The absorbent solution is in a series flow arrangement. The rich-in-water solution leaving the absorber A (state 1) is preheated by the solution heat exchangers and then directly enters the generator G1 (state 13). Now the rich-in-water solution will be gradually concentrated in salt in the different generators G1, G2 and CG (states 14, 23 and 6, respectively).

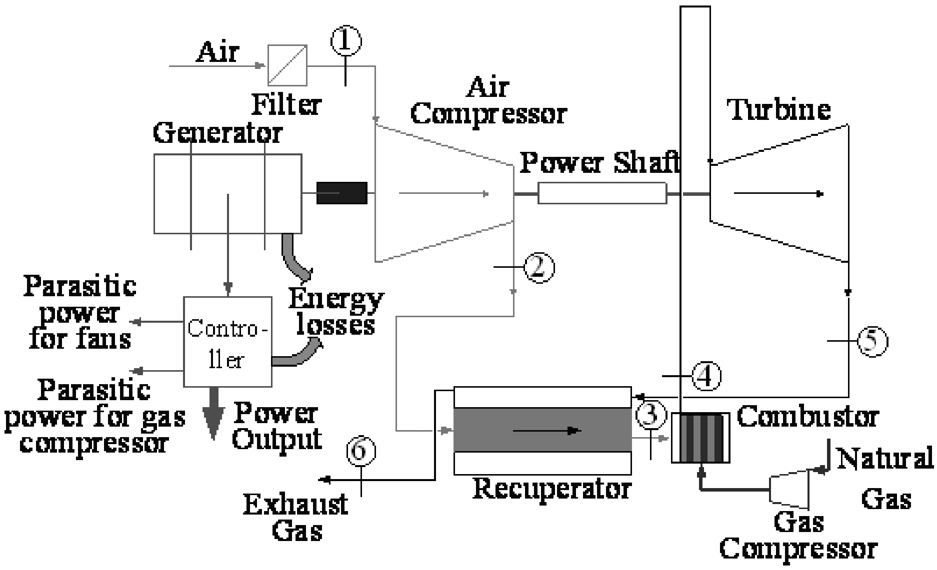


*Figure 3. Schematic of the microturbine generator process.*

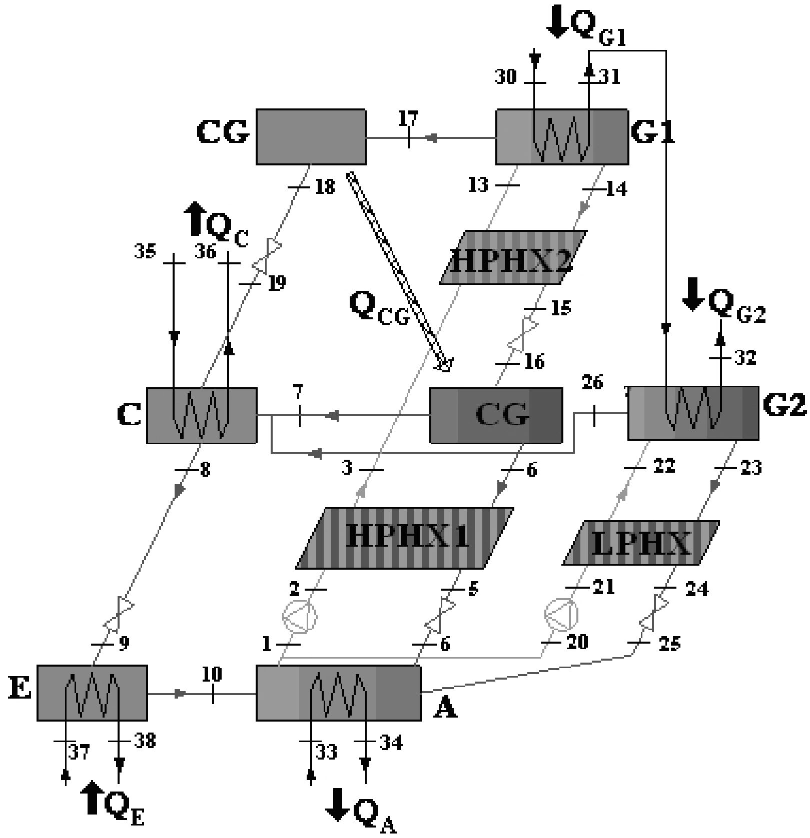


*Figure 4. Components, state points and heat exchanges of a single-double effect absorption cycle.*

TABLE I. ABBREVIATIONS USED IN FIGURE 4.

| Abbreviation | Complete Name | Belongs to |
|---|---|---|
| A | Absorber | Single-double effect cycles |
| C | Condenser | Single-double effect cycles |
| CG | Condenser-Generator | Double effect |
| E | Evaporator | Single-double effect cycles |
| G1 | High Pressure Generator | Double effect |
| G2 | Low Pressure Generator | Single effect |
| HPHX1 | High pressure solution heat exchanger 1 | Double effect |
| HPHX2 | High pressure solution heat exchanger 2 | Double effect |
| LPHX | Low pressure solution heat exchanger | Single effect |

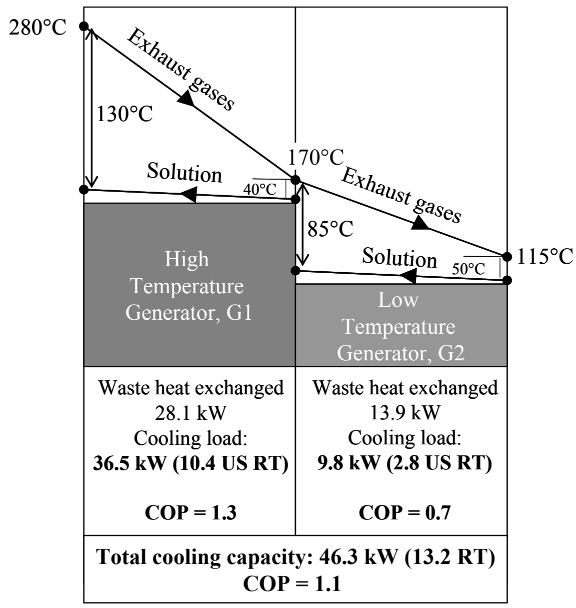


*Figure 5. Temperature distribution and heat exchanged of exhaust gases in the two generators of the EGT15 chiller.*

### 4.2 Chiller simulation methodology

A computer code for the simulation of the cycle has been established using the program EES. Properties for water-LiBr are integrated in EES, except the specific entropy, which has been calculated following Kaita (2001). The specific exergy calculation is given by Misra et al. (2003).

Some input parameters in the model coincide with the experimental variables that will be controlled in the experimental testing phase. Others such as mass exchange efficiencies along with heat transfer coefficients for the suite of heat exchangers comprising the cycle are determined from proprietary manufacturer's testing data at nominal conditions and are assumed constant for the studied working range. The list of input variables of the model is presented below:

- Inlet temperatures and flow rates of external fluids.
- Temperature difference for subcooling in condensers and superheating in evaporator.
- Overall heat transfer coefficients in heat and mass exchangers.
- Mass exchange efficiencies, $\eta_m$, defined as:

$$\eta_m = \frac{X_{out} - X_{in}}{X_{eq,out}(T_{out}, P_{out}) - X_{in}} \tag{1}$$

- Percentage of heat loss in exhaust gas-driven generators, $\alpha$.
- Ratio of outlet absorber solution flow rate to double effect cycle over flow rate to single effect cycle, *f*.

The same type of output data for each state point presented above for the MTG model are also obtained for the chiller model. The principal performance parameter for the absorption chiller is the COP. This parameter is defined as the ratio of cooling produced over driving heat supplied by exhaust gases in generators G1 and G2:

$$COP = \frac{Q_E}{Q_{G1} + Q_{G2}} \tag{2}$$

Principal assumptions of the chiller thermodynamic model are:

- The refrigerant vapor leaving the evaporator is pure water.
- Exhaust gas fired generators operate in cross-current flow.
- No liquid carryover from evaporator
- The solution and refrigerant valves are adiabatic
- No heat losses
- No pressure losses

### 5. Exergy Anaysis

Assessment of overall IES efficiency based on exergy efficiency is recommended (Bejan et al., 1996; Kotas, 1995), as this approach takes into account the disparate energy qualities of the driving natural gas chemical energy, the electric power generated in the MTG, and the cooling produced in the single-double effect absorption chiller. The exergy efficiency is defined as the useful exergy output divided by the exergy input, enabling us to compare cycles with different types of energy inputs. For the selected IES the exergy efficiency can be expressed as:

$$\Psi_{IES} = \frac{\dot{E}_{chw} + \dot{E}_{MTG}}{\dot{E}_{fuel}} = \frac{m_{chw}(e_{out} - e_{in})_{chw} + W_{MTG}}{m_{fuel} LHV \cdot 1.04} \quad (3)$$

The expression for exergy flow of natural gas ($\dot{E}_{fuel}$) is taken from Kotas (1995).

## 6. Results and Discussion

MTG model results show good agreement with manufacturer's nominal values at full load and with literature experimental values at part load performance (Labinov et al., 2002). *Figure 6* shows predicted values for thermal efficiency (based on the HHV of natural gas), and mass flow rate and temperature for the exhaust gases leaving the recuperator, all as a function of MTG net power output. These last two output variables, which characterize the heat content of the waste heat stream, are used as inputs in the chiller model and have a significant effect on the performance of the chiller. As some parasitic losses, such as fan electric motors, are practically independent of power output, thermal efficiency decreases slightly with decreasing power outputs. Both air flow rate and natural gas flow rate (not shown) vary in a fairly linear fashion with MTG output power. The non-linear increase of exhaust gas temperature with output power responds to the empirical correlation of inlet turbine temperature as a function of power used as an input to the model.

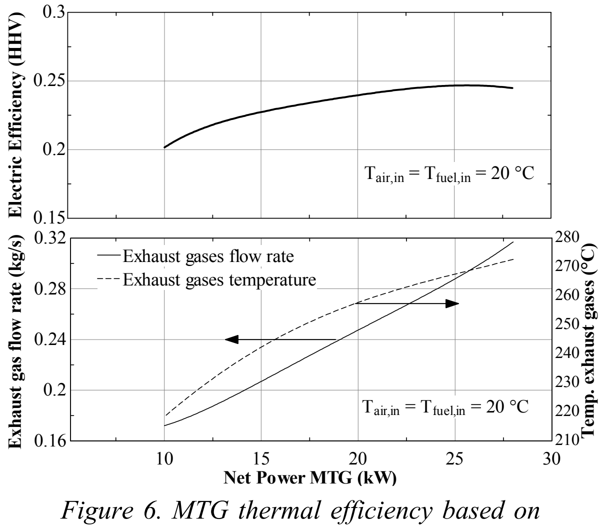


*Figure 6. MTG thermal efficiency based on HHV (above) and exhaust gases flow rate and temperature (below) versus net MTG power output.*

The MTG model also predicts well the expected reduction in thermal efficiency with an increase in ambient air temperature (not shown).

*Figure 7* presents predicted results for chiller cooling capacity and coefficient of performance as a function of inlet chilled water temperature when the MTG is operating at full load and cooling water temperature is at nominal conditions. Similarly, *Figure 8* shows how the same performance parameters are affected by inlet cooling water temperature. An increase of inlet chilled water temperature with constant intermediate level temperature or a decrease of inlet cooling water temperature with constant low temperature level both result in higher COPs and higher cooling capacities. This is due to the decrease in the temperature lift between low and intermediate temperature levels, which is thermodynamically more favorable. As the inlet chilled water temperature decreases, the evaporation temperature and pressure will decrease. Therefore the absorber pressure will decrease and less refrigerant can be absorbed. This implies a decrease of concentration difference between weak and strong solution. In order to maintain the cooling capacity, if the concentration difference decreases, the solution flow ratio has to be increased. An increasing solution flow rate will increase the necessary heat supply to the generator and as a consequence the COP will decrease. An increase of the inlet cooling water temperature will increase condenser temperature and pressure as well as absorber temperature. At a higher condenser pressure less refrigerant can be desorbed in the generator, and at a higher absorber temperature less refrigerant can be absorbed in the absorber. Both effects will decrease the concentration difference between weak and strong solution, increase the solution flow rate and decrease the COP. The study of the effect of cooling water temperature is limited to values above 26.5°C as

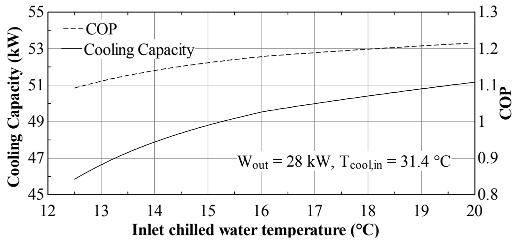


*Figure 7. Effect of chilled water inlet temperature on chiller cooling capacity and on COP for full load MTG conditions.*

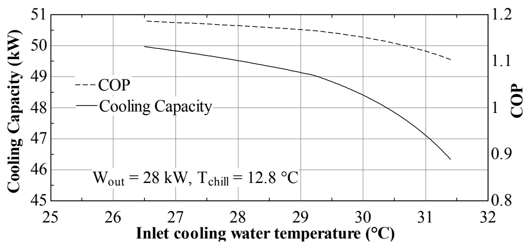


*Figure 8: Effect of cooling water inlet temperature on chiller cooling capacity and on COP for full load MTG conditions.*

lower temperatures lead to crystallization of LiBr for the solution streams at the absorber inlet (state points 5 and 24 in *Figure 4*).

Unlike the MTG model, which includes empirical correlations of some parameters to account for the control strategy of the real unit, these types of correlations are not available for the chiller model. This means that the model is predicting how the chiller would behave if no controls had been implemented. For that reason predicted results for chiller performance at part load MTG operating conditions (*Figure 9*) are restricted to a very narrow range (25.6-28 kW). With mass flow rates and temperatures of the exhaust gases corresponding to MTG loads below 25.6 kW, the model predicts crystallization will occur at solution stream 24, which leaves the solution heat exchanger of the single effect cycle. The control devices implemented in the real unit prevent crystallization by changing flow rates and, according to manufacturer's data, should enable some cooling production at MTG part load performances as low as 15 kW. However, *Figure 9* estimates correctly the expected trends of decreasing cooling capacity with decreasing MTG power output.

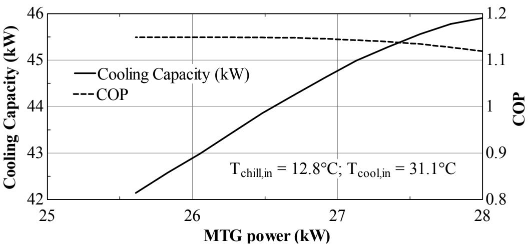


*Figure 9. Effect of MTG power output on chiller cooling capacity and on COP.*

Energy efficiencies have been assessed individually for the MTG cycle and the absorption cycle that integrate the IES presented in this study. The exergy efficiency is applied to compare overall efficiencies of three similar IESs that vary in the configuration of the chiller. The chiller absorption cycles chosen are the single-double effect studied in this work, the single effect cycle and the double effect cycle. The MTG power is the same for the three IESs. TABLE II presents exergy results for the three IES configurations. As expected, the IES with the novel single-double effect absorption cycle is the one with the highest overall exergy efficiency, as it produces the largest cooling for the same amount of natural gas driving energy.

## 7. Conclusions

A theoretical analysis of a commercial integrated energy system consisting of a microturbine and an absorption chiller was presented as a first step for planning and executing performance tests of the real unit at the APEP DG-IES test facility. Steady-state models for the MTG and the chiller were developed and results analyzed. The principal findings of this study are:

The MTG model predicts that the thermal efficiency, as well as the exhaust gas flow rate and temperature, increase with power output, in good agreement with published experimental data.

TABLE II. DETERMINATION OF OVERALL IES EXERGY EFFICIENCIES WITH THREE DIFFERENT CYCLE CONFIGURATIONS FOR THE ABSORPTION CHILLER.

| | IES with Single-Double effect chiller | IES with Double effect chiller | IES with Single effect chiller |
|---|---|---|---|
| $m_{fuel}$ (kg/s) | 0.0027 | 0.0027 | 0.0027 |
| $\dot{E}_{fuel}$ (kW) | 106.6 | 106.6 | 106.6 |
| $\dot{E}_{MTG}$ (kW) | 28 | 28 | 28 |
| Cooling (kW)* | 46.2 | 37.6 | 29.4 |
| $\dot{E}_{chw}$ (kW) | 2.35 | 1.91 | 1.49 |
| $\Psi_{IES}$ | 0.285 | 0.281 | 0.277 |

* Cooling refers to an energy flow and not to an exergy flow.

The absorption chiller model predicts the increase of COP and cooling capacity with increasing chilled water temperatures and decreasing cooling water temperatures, with maximum COPs above 1.2.

Part load performance of the chiller is not accurately represented by the current model. The absorption chiller model should be improved with empirical correlations obtained in the future test phase to take into account chiller crystallization and part load controls.

The overall exergy efficiency of the studied IES with the novel chiller using a single-double effect absorption cycle is higher than the ones resulting from the same MTG and exhaust gas fired single or double effect chillers.

The second part of this project is the actual performance evaluation of the commercial IES. Preliminary results of this test phase will be presented in a following paper.

**Nomenclature**

| | |
|---|---|
| $\dot{E}$ | Exergy flow (kW) |
| e | Exergy (kJ) |
| HHV | Higher Heating Value (kJ/kg) |
| LHV | Lower Heating Value (kJ/kg) |
| m | Mass flow rate (kg/s) |
| Q | Heat power (kW) |
| P | Pressure (kPa) |

| | |
|---|---|
| T | Temperature (°C) |
| X | LiBr solution concentration (kg/kg) |
| W | Power (kW) |

**Greek letters**

| | |
|---|---|
| $\Psi$ | Exergy efficiency of the cycle (-) |
| $\eta$ | Efficiency (-) |

**Indices**

| | |
|---|---|
| chw | Chilled water |
| eq | Equilibrium conditions |
| E | Evaporator |
| G1 | Generator at high temperature |
| G2 | Generator at low temperature |
| in | Inlet |
| m | Mass |
| out | Outlet |

**References**


Bejan, A., Tsatsaronis, G. and Moran, M., 1996, *Thermal Design & Optimization*, New York, John Wiley & Sons Inc.

Engle, D., 2004, "The New Trigeneration Players: Integrated Cooling, Heating and Power Systems are Here", *Distributed Energy, The Journal for Onsite Power Solutions*, http://www.distributedenergy.com/de_0405_trigeneration.html

Gillette, S., 2004, "Microturbine Advances", *Globalcon*, March 24-25, Boston, MA.

Herold, H., Radermacher, R., Klein, SA, 1996, *Absorption chillers and heat pumps,* CRC Press, Boca Raton, Florida.

Kaita, Y., 2001, "Thermodynamic properties of lithium bromide-water solutions at high temperatures", *International Journal of Refrigeration* , Vol. 24, pp. 374-390.

Kotas, T., 1995, *The Exergy Method of Thermal Plant Analysis*, Melbourne, Florida, Krieger Publishing Company.

Labinov, S. D, Zaltash, A., Rizy, D. T., Fairchild, P. D., Robert, P. E., DeVault, R. D., Vineyard, E. A., 2002, "Predictive Algorithms for Microturbine Performance for BCHP Systems". *ASHRAE Transactions of the Annual Meeting*, vol. 108, pp.1-9, paper HI-02-5-3.

McDonell, V. G, Hack, R. L, Lee, S. W., Mauzey, J. L., Wojciechowski, J.S., Samuelsen, G. S., 2003, "Experiences with Microturbine generators systems installed in the South Coast Air Quality Management District", *TURBOEXPO 2003-Land, Sea, and Air, 49th ASME International Gas Turbine & Aeroengine Technical Congress,* Atlanta, Georgia.

Misra, R. D., Sahoo, P. K., Sahoo, S. and Gupta, A., 2003, "Thermoeconomic optimization of a single effect water/LiBr vapour absorption refrigeration system," *International Journal of Refrigeration*, Vol. 26, No. 2, pp. 158-169.

Nogués, M., Mauzey, J., Freeman, A., McDonell, V., Samuelsen, S. "Experimental Results of a Novel Integrated Energy System Formed by a Microturbine and an Exhaust Fired Single-Double Effect Absorption Chiller", *TURBOEXPO 2006 Power for Land, Sea, and Air, 51st ASME International Gas Turbine & Aeroengine Technical Congress,* Barcelona, Spain, paper GT2006-91264.